46. M. A. J. Chaplain, T. Lorenzi and F. R. Macfarlane, Bridging the gap between individual-based and continuum models of growing cell populations, *J. Math. Biol.*, **80** (2020), 342–371.
47. M. Inoue, Derivation of a porous medium equation from many markovian particles and the propagation of chaos, *Hiroshima Math. J.*, **21** (1991), 85–110.
48. K. Oelschläger, On the derivation of reaction-diffusion equations as limit dynamics of systems of moderately interacting stochastic processes, *Probab. Theory Relat. Fields*, **82** (1989), 565–586.
49. H. G. Othmer and T. Hillen, The diffusion limit of transport equations II: Chemotaxis equations, *SIAM J. Appl. Math.*, **62** (2002), 1222–1250.
50. C. J. Penington, B. D. Hughes and K. A. Landman, Building macroscale models from microscale probabilistic models: A general probabilistic approach for nonlinear diffusion and multispecies phenomena, *Phys. Rev. E*, **84** (2011), 041120.
51. C. J. Penington, B. D. Hughes and K. A. Landman, Interacting motile agents: Taking a mean-field approach beyond monomers and nearest-neighbor steps, *Phys. Rev. E*, **89** (2014), 032714.
52. R. E. Baker, A. Parker and M. J. Simpson, A free boundary model of epithelial dynamics, *J. Theor. Biol.*, **481** (2019), 61–74.
53. H. M. Byrne and D. Drasdo, Individual-based and continuum models of growing cell populations: A comparison, *J. Math. Biol.*, **58** (2009), 657.
54. T. Lorenzi, P. J. Murray and M. Ptashnyk, From individual-based mechanical models of multicellular systems to free-boundary problems, *Interface Free Bound.*, **22** (2020), 205–244.
55. S. Motsch and D. Peurichard, From short-range repulsion to hele-shaw problem in a model of tumor growth, *J. Math. Biol.*, **76** (2018), 205–234.
56. P. J. Murray, C. M. Edwards, M. J. Tindall and P. K. Maini, From a discrete to a continuum model of cell dynamics in one dimension, *Phys. Rev. E*, **80** (2009), 031912.
57. P. J. Murray, C. M. Edwards, M. J. Tindall and P. K. Maini, Classifying general nonlinear force laws in cell-based models via the continuum limit, *Phys. Rev. E*, **85** (2012), 021921.
58. K. Oelschläger, Large systems of interacting particles and the porous medium equation, *J. Diff. equation.*, **88** (1990), 294–346.
59. B. J. Binder and K. A. Landman, Exclusion processes on a growing domain, *J. Theor. Biol.*, **259** (2009), 541–551.
60. L. Dyson, P. K. Maini and R. E. Baker, Macroscopic limits of individual-based models for motile cell populations with volume exclusion, *Phys. Rev. E*, **86** (2012), 031903.
61. A. E. Fernando, K. A. Landman and M. J. Simpson, Nonlinear diffusion and exclusion processes with contact interactions, *Phys. Rev. E*, **81** (2010), 011903.
62. S. T. Johnston, R. E. Baker, D. S. McElwain and M. J. Simpson, Co-operation, competition and crowding: a discrete framework linking allee kinetics, nonlinear diffusion, shocks and sharp-fronted travelling waves, *Sci. Rep.*, **7** (2017), 42134.
63. S. T. Johnston, M. J. Simpson and R. E. Baker, Mean-field descriptions of collective migration with strong adhesion, *Phys. Rev. E*, **85** (2012), 051922.
64. K. A. Landman and A. E. Fernando, Myopic random walkers and exclusion processes: Single and multispecies, *Phys. A Stat. Mech. Appl.*, **390** (2011), 3742–3753.
65. P. M. Lushnikov, N. Chen and M. Alber, Macroscopic dynamics of biological cells interacting via chemotaxis and direct contact, *Phys. Rev. E*, **78** (2008), 061904.

66. M. J. Simpson, K. A. Landman and B. D. Hughes, Cell invasion with proliferation mechanisms motivated by time-lapse data, *Phys. A Stat. Mech. Appl.*, **389** (2010), 3779–3790.
67. C. Deroulers, M. Aubert, M. Badoual and B. Grammaticos, Modeling tumor cell migration: from microscopic to macroscopic models, *Phys. Rev. E*, **79** (2009), 031917.
68. D. Drasdo, Coarse graining in simulated cell populations, *Adv. Complex Syst.*, **8** (2005), 319–363.
69. M. J. Simpson, A. Merrifield, K. A. Landman and B. D. Hughes, Simulating invasion with cellular automata: connecting cell-scale and population-scale properties, *Phys. Rev. E*, **76** (2007), 021918.
70. A. Buttenschoen, T. Hillen, A. Gerisch and K. J. Painter, A space-jump derivation for non-local models of cell–cell adhesion and non-local chemotaxis, *J. Math. Biol.*, **76** (2018), 429–456.
71. L. Marcon and J. Sharpe, Turing patterns in development: What about the horse part? *Curr. Opin. Genet. Dev.*, **22** (2012), 578–584.
72. H. G. Othmer, P. K. Maini and J. D. Murray, *Experimental and theoretical advances in biological pattern formation*, vol. 259, Springer Science & Business Media, 2012.
73. H. G. Othmer, K. J. Painter, D. Umulis, and C. Xue, The intersection of theory and application in elucidating pattern formation in developmental biology, *Math. Model. Nat. Phenom.*, **4** (2009), 3–82.
74. P. Maini, K. Painter and H. P. Chau, Spatial pattern formation in chemical and biological systems, *J. Chem. Soc. Faraday Trans.*, **93** (1997), 3601–3610.
75. M. R. Myerscough, P. K. Maini, and K. J. Painter, Pattern formation in a generalized chemotactic model, *Bull. Math. Biol.*, **60** (1998), 1–26.
76. J. A. Sherratt and J. D. Murray, Mathematical analysis of a basic model for epidermal wound healing, *J. Math. Biol.*, **29** (1991), 389–404.
77. J. Schnakenberg, Simple chemical reaction systems with limit cycle behaviour, *J. Theor. Biol.*, **81** (1979), 389–400.
78. G. Lolas, *Spatio-temporal pattern formation and reaction diffusion systems*, Master's thesis, University of Dundee Scotland, 1999.
79. R. McLennan, L. Dyson, K. W. Prather, J. A. Morrison, R. E. Baker, P. K. Maini, and P. M. Kulesa, Multiscale mechanisms of cell migration during development: Theory and experiment, *Development*, **139** (2012), 2935–2944.
80. R. McLennan, L. J. Schumacher, J. A. Morrison, J. M. Teddy, D. A. Ridenour, A. C. Box, C. L. Semerad, H. Li, W. McDowell, D. Kay, et al, Neural crest migration is driven by a few trailblazer cells with a unique molecular signature narrowly confined to the invasive front, *Development*, **142** (2015), 2014–2025.
81. R. McLennan, L. J. Schumacher, J. A. Morrison, J. M. Teddy, D. A. Ridenour, A. C. Box, C. L. Semerad, H. Li, W. McDowell, D. Kay, et al, VEGF signals induce trailblazer cell identity that drives neural crest migration, *Dev. Biol.*, **407** (2015),12–25.
82. J. D. Murray, G. F. Oster, and A. K. Harris, A mechanical model for mesenchymal morphogenesis, *J. Math. Biol.*, **17** (1983), 125–129.
83. F. Schweisguth and F. Corson, Self-organization in pattern formation, *Develop. Cell*, **49** (2019), 659–677.
84. L. Tweedy, D. A. Knecht, G. M. Mackay, and R. H. Insall, Self-generated chemoattractant gradients: attractant depletion extends the range and robustness of chemotaxis, *PLoS Biol.*, **14** (2016), e1002404.

85. J. Galle, M. Loeffler, and D. Drasdo, Modeling the effect of deregulated proliferation and apoptosis on the growth dynamics of epithelial cell populations in vitro, *Biophys. J.*, **88** (2005), 62–75.
86. J. Galle, G. Aust, G. Schaller, T. Beyer, and D. Drasdo, Individual cell-based models of the spatial-temporal organization of multicellular systems—Achievements and limitations, *Cytom. A*, **69** (2006), 704–710.
87. D. Drasdo, S. Hoehme, and M. Block, On the role of physics in the growth and pattern formation of multi-cellular systems: What can we learn from individual-cell based models? *J. Stat. Phys.*, **128** (2007), 287.
88. M. P. Neilson, D. M. Veltman, P. J. M. van Haastert, S. D. Webb, J. A. Mackenzie, and R. H. Insall, Chemotaxis: A feedback-based computational model robustly predicts multiple aspects of real cell behaviour, *PLoS Biol.*, **9** (2011), e1000618.
89. S. Kondo, An updated kernel-based turing model for studying the mechanisms of biological pattern formation, *J. Theor Biol.*, **414** (2017), 120–127.

Appendix

A. Formal derivation of the deterministic continuum model on growing domains

We carry out a formal derivation of the deterministic continuum model given by the PDE (2.16) for $d = 2$. Similar methods can be used in the case where $d = 1$.

When cell dynamics are governed by the rules described in Section 2.1.2 and Section 3.1.2, considering $(i, j) \in [1, I-1] \times [1, I-1]$, the mass balance principle gives

$$\begin{aligned}
n^{k+1}_{(i,j)} \;=\;& n^k_{(i,j)} + \frac{\theta}{4\mathcal{L}_k^2}\Big[n^k_{(i+1,j)} + n^k_{(i-1,j)} + n^k_{(i,j+1)} + n^k_{(i,j-1)} - 4n^k_{(i,j)}\Big] \\
&+ \frac{\eta}{4\,u_{\max}\mathcal{L}_k^2}\Big[\Big(u^k_{(i,j)} - u^k_{(i-1,j)}\Big)_+ n^k_{(i-1,j)} + \Big(u^k_{(i,j)} - u^k_{(i+1,j)}\Big)_+ n^k_{(i+1,j)}\Big] \\
&+ \frac{\eta}{4\,u_{\max}\mathcal{L}_k^2}\Big[\Big(u^k_{(i,j)} - u^k_{(i,j-1)}\Big)_+ n^k_{(i,j-1)} + \Big(u^k_{(i,j)} - u^k_{(i,j+1)}\Big)_+ n^k_{(i,j+1)}\Big] \\
&- \frac{\eta}{4\,u_{\max}\mathcal{L}_k^2}\Big[\Big(u^k_{(i-1,j)} - u^k_{(i,j)}\Big)_+ + \Big(u^k_{(i+1,j)} - u^k_{(i,j)}\Big)_+\Big] n^k_{(i,j)} \\
&- \frac{\eta}{4\,u_{\max}\mathcal{L}_k^2}\Big[\Big(u^k_{(i,j-1)} - u^k_{(i,j)}\Big)_+ + \Big(u^k_{(i,j+1)} - u^k_{(i,j)}\Big)_+\Big] n^k_{(i,j)} \\
&+ \tau\Big(\alpha_n \psi(n^k_{(i,j)})\phi_u(u^k_{(i,j)}) - \beta_n \phi_v(v^k_{(i,j)})\Big) n^k_{(i,j)} - g_{(i,j)}(n^k_{(i,j)}, \mathcal{L}_k).
\end{aligned} \tag{A.1}$$

Using the fact that the following relations hold for τ and χ sufficiently small

$$\begin{gathered}
t_k \approx t, \quad t_{k+1} \approx t + \tau, \quad \hat{x}_i \approx \hat{x}, \quad \hat{x}_{i\pm1} \approx \hat{x} \pm \chi, \quad \hat{y}_j \approx \hat{y}, \quad \hat{y}_{j\pm1} \approx \hat{y} \pm \chi \\
n^k_{(i,j)} \approx n(t, \hat{x}, \hat{y}), \quad n^{k+1}_{(i,j)} \approx n(t+\tau, \hat{x}, \hat{y}), \quad n^k_{(i\pm1,j)} \approx n(t, \hat{x} \pm \chi, \hat{y}), \quad n^k_{(i,j\pm1)} \approx n(t, \hat{x}, \hat{y} \pm \chi), \\
u^k_{(i,j)} \approx u(t, \hat{x}, \hat{y}), \quad u^{k+1}_{(i,j)} \approx u(t+\tau, \hat{x}, \hat{y}), \quad u^k_{(i\pm1,j)} \approx u(t, \hat{x} \pm \chi, \hat{y}), \quad u^k_{(i,j\pm1)} \approx u(t, \hat{x}, \hat{y} \pm \chi), \\
v^k_{(i,j)} \approx v(t, \hat{x}, \hat{y}), \quad v^{k+1}_{(i,j)} \approx v(t+\tau, \hat{x}, \hat{y}), \quad v^k_{(i\pm1,j)} \approx v(t, \hat{x} \pm \chi, \hat{y}), \quad v^k_{(i,j\pm1)} \approx v(t, \hat{x}, \hat{y} \pm \chi), \\
\mathcal{L}_k \approx \mathcal{L}(t), \quad \mathcal{L}_{k+1} \approx \mathcal{L}(t+\tau),
\end{gathered}$$

the balance equation (A.1) can be formally rewritten in the approximate form

$$
\begin{aligned}
n(t+\tau,\hat{x},\hat{y}) \;=\;& n+\frac{\theta}{4\mathcal{L}^2}\Big[n(t,\hat{x}+\chi,\hat{y})+n(t,\hat{x}-\chi,\hat{y})+n(t,\hat{x},\hat{y}+\chi)+n(t,\hat{x},\hat{y}-\chi)-4n\Big]\\
&+\frac{\eta}{4\,u_{\max}\mathcal{L}^2}\Big[\Big(u-u(t,\hat{x}-\chi,\hat{y})\Big)_+\,n(t,\hat{x}-\chi,\hat{y})+\Big(u-u(t,\hat{x}+\chi,\hat{y})\Big)_+\,n(t,\hat{x}+\chi,\hat{y})\Big]\\
&+\frac{\eta}{4\,u_{\max}\mathcal{L}^2}\Big[\Big(u-u(t,\hat{x},\hat{y}-\chi)\Big)_+\,n(t,\hat{x},\hat{y}-\chi)+\Big(u-u(t,\hat{x},\hat{y}+\chi)\Big)_+\,n(t,\hat{x},\hat{y}+\chi)\Big]\\
&-\frac{\eta}{4\,u_{\max}\mathcal{L}^2}\Big[\Big(u(t,\hat{x}-\chi,\hat{y})-u\Big)_++\Big(u(t,\hat{x}+\chi,\hat{y})-u\Big)_+\Big]n\\
&-\frac{\eta}{4\,u_{\max}\mathcal{L}^2}\Big[\Big(u(t,\hat{x},\hat{y}-\chi)-u\Big)_++\Big(u(t,\hat{x},\hat{y}+\chi)-u\Big)_+\Big]n\\
&+\tau\Big(\alpha_n\psi(n)\phi_u(u)-\beta_n\phi_v(v)\Big)n-\Gamma\left(\hat{x},\hat{y},n,\mathcal{L}\right),
\end{aligned}
\tag{A.2}
$$

with

$$
\Gamma\left(\hat{x},\hat{y},n,\mathcal{L}\right):=\begin{cases}
2\,n\,\dfrac{\mathcal{L}(t+\tau)-\mathcal{L}(t)}{\mathcal{L}(t)}, & \text{if } g_{(i,j)}(n^k_{(i,j)}) \text{ is defined via Eq (3.3),}\\[2ex]
\left[\dfrac{\hat{x}}{\chi}\Big(n(t,\hat{x}+\chi,\hat{y})-n\Big)+\dfrac{\hat{y}}{\chi}\Big(n(t,\hat{x},\hat{y}+\chi)-n\Big)\right]\dfrac{\mathcal{L}(t+\tau)-\mathcal{L}(t)}{\mathcal{L}(t)}, & \text{if } g_{(i,j)}(n^k_{(i,j)}) \text{ is defined via Eq (3.4),}
\end{cases}
$$

where $n\equiv n(t,\hat{x},\hat{y})$, $u\equiv u(t,\hat{x},\hat{y})$, $v\equiv v(t,\hat{x},\hat{y})$ and $\mathcal{L}\equiv\mathcal{L}(t)$. Dividing both sides of Eq (A.2) by τ gives

$$
\begin{aligned}
\frac{n(t+\tau,\hat{x},\hat{y})-n}{\tau} \;=\;& \frac{\theta}{4\mathcal{L}^2\tau}\Big[n(t,\hat{x}+\chi,\hat{y})+n(t,\hat{x}-\chi,\hat{y})+n(t,\hat{x},\hat{y}+\chi)+n(t,\hat{x},\hat{y}-\chi)-4n\Big]\\
&+\frac{\eta}{4\,u_{\max}\mathcal{L}^2\tau}\Big[\Big(u-u(t,\hat{x}-\chi,\hat{y})\Big)_+\,n(t,\hat{x}-\chi,\hat{y})+\Big(u-u(t,\hat{x}+\chi,\hat{y})\Big)_+\,n(t,\hat{x}+\chi,\hat{y})\Big]\\
&+\frac{\eta}{4\,u_{\max}\mathcal{L}^2\tau}\Big[\Big(u-u(t,\hat{x},\hat{y}-\chi)\Big)_+\,n(t,\hat{x},\hat{y}-\chi)+\Big(u-u(t,\hat{x},\hat{y}+\chi)\Big)_+\,n(t,\hat{x},\hat{y}+\chi)\Big]\\
&-\frac{\eta}{4\,u_{\max}\mathcal{L}^2\tau}\Big[\Big(u(t,\hat{x}-\chi,\hat{y})-u\Big)_++\Big(u(t,\hat{x}+\chi,\hat{y})-u\Big)_+\Big]n\\
&-\frac{\eta}{4\,u_{\max}\mathcal{L}^2\tau}\Big[\Big(u(t,\hat{x},\hat{y}-\chi)-u\Big)_++\Big(u(t,\hat{x},\hat{y}+\chi)-u\Big)_+\Big]n\\
&+\Big(\alpha_n\psi(n)\phi_u(u)-\beta_n\phi_v(v)\Big)n-\frac{1}{\tau}\Gamma\left(\hat{x},\hat{y},n,\mathcal{L}\right).
\end{aligned}
\tag{A.3}
$$

If $n(t,\hat{x},\hat{y})$ is a twice continuously differentiable function of $\hat{x}$ and $\hat{y}$ and a continuously differentiable function of t, $u(t,\hat{x},\hat{y})$ is a twice continuously differentiable function of $\hat{x}$ and $\hat{y}$, and the function $\mathcal{L}(t)$ is continuously differentiable, for χ and τ sufficiently small we can use the Taylor expansions

$$
n(t,\hat{x}\pm\chi,\hat{y})=n\pm\chi\frac{\partial n}{\partial\hat{x}}+\frac{\chi^2}{2}\frac{\partial^2 n}{\partial\hat{x}^2}+O(\chi^3),\quad n(t,\hat{x},\hat{y}\pm\chi)=n\pm\chi\frac{\partial n}{\partial\hat{y}}+\frac{\chi^2}{2}\frac{\partial^2 n}{\partial\hat{y}^2}+O(\chi^3),
$$

$$
n(t+\tau,\hat{x},\hat{y})=n+\tau\frac{\partial n}{\partial t}+O(\tau^2),
$$

$$
u(t,\hat{x}\pm\chi,\hat{y})=u\pm\chi\frac{\partial u}{\partial\hat{x}}+\frac{\chi^2}{2}\frac{\partial^2 u}{\partial\hat{x}^2}+O(\chi^3),\quad u(t,\hat{x},\hat{y}\pm\chi)=u\pm\chi\frac{\partial u}{\partial\hat{y}}+\frac{\chi^2}{2}\frac{\partial^2 u}{\partial\hat{y}^2}+O(\chi^3),
$$

$$\mathcal{L}(t+\tau) = \mathcal{L} + \tau \frac{\mathrm{d}\mathcal{L}}{\mathrm{d}t} + O(\tau^2).$$

Substituting into Eq (A.3), using the elementary property $(a)_+ - (-a)_+ = a$ for $a \in \mathbb{R}$ and letting $\tau \to 0$ and $\chi \to 0$ in such a way that conditions (2.16) are met, after a little algebra, as similarly done in [44], we find

$$\begin{aligned} \frac{\partial n}{\partial t} &= \frac{D_n}{\mathcal{L}^2}\left(\frac{\partial^2 n}{\partial \hat{x}^2} + \frac{\partial^2 n}{\partial \hat{y}^2}\right) + \frac{C_n}{\mathcal{L}^2}\left[\left(\frac{\partial^2 u}{\partial \hat{x}^2} + \frac{\partial^2 u}{\partial \hat{y}^2}\right) n - \left(\frac{\partial u}{\partial \hat{x}}\frac{\partial n}{\partial \hat{x}} + \frac{\partial u}{\partial \hat{y}}\frac{\partial n}{\partial \hat{y}}\right)\right] \\ &\quad + \Big(\alpha_n \psi(n)\phi_u(u) - \beta_n \phi_v(v)\Big) n - G(\hat{x}, \hat{y}, n, \mathcal{L}), \quad (t, \hat{x}, \hat{y}) \in \mathbb{R}_+^* \times (0,1) \times (0,1), \end{aligned} \tag{A.4}$$

where $G(\hat{x}, \hat{y}, n, \mathcal{L})$ is given by Eq (3.13) in the case where $g_{(i,j)}(n^k_{(i,j)})$ is defined via Eq (3.3) and by equation (3.14) in the case where $g_{(i,j)}(n^k_{(i,j)})$ is defined via Eq (3.4). The PDE (A.4) can be easily rewritten in the form of Eq (3.12). Moreover, zero-flux boundary conditions easily follow from the fact that [*cf.* definitions (3.5)–(3.8)]

$$\mathcal{T}^k_{\mathrm{L}(0,j)} := 0, \quad \mathcal{T}^k_{\mathrm{R}(I,j)} := 0, \quad \mathcal{J}^k_{\mathrm{L}(0,j)} := 0, \quad \mathcal{J}^k_{\mathrm{R}(I,j)} := 0 \quad \text{for } j \in [0, I]$$

and

$$\mathcal{T}^k_{\mathrm{D}(i,0)} := 0, \quad \mathcal{T}^k_{\mathrm{U}(i,I)} := 0, \quad \mathcal{J}^k_{\mathrm{D}(i,0)} := 0, \quad \mathcal{J}^k_{\mathrm{U}(i,I)} := 0 \quad \text{for } i \in [0, I].$$

Remark A.1. *The derivation of the continuum limit for the static domain case can be carried out in a similar way by assuming $\mathcal{L}_k$ to be constant, which implies that $g_{\mathbf{i}} \equiv 0$ and results in $G \equiv 0$.*

B. Set-up of numerical simulations on static domains

We let $x \in [0,1]$, $y \in [0,1]$ and $\chi := 0.005$ (*i.e.*, $I = 201$). Moreover, we define $\tau := 1 \times 10^{-3}$.

Dynamics of the morphogens For the dynamics of the morphogens, we consider the parameter setting used in [13], that is,

$$D_u := 1 \times 10^{-4}, \quad D_v := 4 \times 10^{-3}, \quad \alpha_u := 0.1, \quad \beta := 1, \quad \gamma := 1, \quad \alpha_v := 0.9. \tag{B.1}$$

Moreover, we assume the initial distributions to be small perturbations of the homogeneous steady state $(u^*, v^*) \equiv (1, 0.9)$, that is,

$$u^0_{\mathbf{i}} = u^* - \rho + 2\rho\,\mathbf{R} \quad \text{and} \quad v^0_{\mathbf{i}} = v^* - \rho + 2\rho\,\mathbf{R}$$

where $\rho := 0.001$ and $\mathbf{R}$ is either a vector for $d = 1$ or a matrix for $d = 2$ whose components are random numbers drawn from the standard uniform distribution on the interval $(0,1)$, using the built-in Matlab function rand. These choices of the initial distributions of morphogens are such that

$$u^* - \rho \le u^0_{\mathbf{i}} \le u^* + \rho \quad \text{and} \quad v^* - \rho \le v^0_{\mathbf{i}} \le v^* + \rho \quad \text{for all } \mathbf{i},$$

that is, the parameter ρ determines the level of perturbation from the homogeneous steady state. Since the difference equations (2.2) governing the dynamics of the morphogens are independent from the dynamics of the cells, such equations are solved first for all time-steps and the solutions obtained are then used to evaluate both the probabilities of cell movement [*cf.* definitions (2.6)–(2.9)] and the probabilities of cell division and death [*cf.* definitions (2.11)–(2.13)]. The parameter $u_{\max}$ in definitions (2.8) and (2.9) is defined as $\max\limits_{k,\mathbf{i}} u^k_{\mathbf{i}}$.

Computational implementation of the rules underlying the dynamics of the cells At each time-step, each cell undergoes a three-phase process: Phase 1) undirected, random movement according to the probabilities described in the definitions (2.6) and (2.7); Phase 2) chemotaxis according to the probabilities described via the definitions (2.8) and (2.9); Phase 3) division and death according to the probabilities defined via Eqs (2.11)–(2.13). For each cell, during each phase, a random number is drawn from the standard uniform distribution on the interval $(0, 1)$ using the built-in MATLAB function RAND. It is then evaluated whether this number is lower than the probability of the event occurring and if so the event occurs.

Dynamics of the cells Unless stated otherwise, we assume the initial cell distributions to be homogeneous with

$$n_i^0 \equiv 10^4 \;\text{ when } d = 1 \quad \text{and} \quad n_{\mathbf{i}}^0 \equiv 4 \times 10^5 \;\text{ when } d = 2.$$

In the case where chemically-controlled cell proliferation occurs and there is no chemotaxis, unless stated otherwise, we use the following parameter values when $d = 1$

$$\theta := 0.05, \quad \eta := 0, \quad \alpha_n := 5, \quad \beta_n := 1, \quad n_{\max} := 2 \times 10^4.$$

and the following ones when $d = 2$

$$\theta := 0.005, \quad \eta := 0, \quad \alpha_n := 5, \quad \beta_n := 0.1, \quad n_{\max} := 8 \times 10^5.$$

The results shown in Figures 5 and 6 refer to the same settings with the modification that when $d = 1$

$$n_i^0 \equiv 4 \times 10^3 \quad \text{and} \quad n_{\max} := 1.5 \times 10^3$$

and when $d = 2$

$$n_{\mathbf{i}}^0 \equiv 2 \times 10^5 \quad \text{and} \quad n_{\max} := 8 \times 10^4.$$

In the case where cells undergo chemotaxis and cell proliferation is not chemically-controlled, unless stated otherwise, we use the following parameter values when $d = 1$

$$\theta := 0.05, \quad \eta := 1, \quad \alpha_n := 0.1, \quad \beta_n := 0.055, \quad n_{\max} := 2 \times 10^4.$$

and the following ones when $d = 2$

$$\theta := 0.005, \quad \eta = 1, \quad \alpha_n := 0.1, \quad \beta_n := 0.055, \quad n_{\max} := 8 \times 10^5.$$

Numerical solutions of the corresponding continuum models Numerical solutions of the PDE (2.17) and the system of PDEs (2.18) subject to zero-flux boundary conditions are computed through standard finite-difference schemes using initial conditions and parameter values that are compatible with those used for the IB model and the system of difference equations (2.2). In particular, the values of the parameters D_n and C_n in the PDE (2.17) are described via the definitions (2.23).

C. Set-up of numerical simulations on growing domains

We let $x \in [0, 1]$, $y \in [0, 1]$ and $\chi := 0.005$ (i.e., $I = 201$). Moreover, we assume $\tau := 1 \times 10^{-3}$ and we define $\mathcal{L}$ according to equation (3.16) (i.e., the domain grows linearly over time).

Dynamics of the morphogens For the dynamics of the morphogens, we use the parameter setting given by the definitions (B.1). Moreover, we define the initial distributions as the numerical equilibrium distributions obtained in the case of static domains. Similarly to the case of static domains, since the difference equations (3.2) governing the dynamics of the morphogens are independent from the dynamics of the cells, such equations are solved first for all time-steps and the solutions obtained are then used to evaluate both the probabilities of cell movement given by definitions (3.5)–(3.8) and the probabilities of cell division and death given by Eqs (3.9)–(3.11). The parameter $u_{\max}$ in the definitions (3.7) and (3.8) is defined as $\max_{k,\mathbf{i}} u_{\mathbf{i}}^k$.

Computational implementation of the rules underlying the dynamics of the cells Similarly to the case of static domains, at each time-step, each cell undergoes a three-phase process: Phase 1) undirected, random movement according to the probabilities described through the definitions (3.5) and (3.6); Phase 2) chemotaxis according to the probabilities described through the definitions (3.7) and (3.8); Phase 3) division and death according to the probabilities defined via Eqs (3.9)–(3.11). For each cell, during each phase, a random number is drawn from the standard uniform distribution on the interval $(0, 1)$ using the built-in MATLAB function RAND. It is then evaluated whether this number is lower than the probability of the event occurring and if so the event occurs.

Dynamics of the cells We assume the initial cell distributions and all parameter values to be the same as those used in the static domain case.

Numerical solutions of the corresponding continuum models Numerical solutions of the PDE (3.12) and the system of PDEs (3.15) subject to zero-flux boundary conditions are computed through standard finite-difference schemes using initial conditions and parameter values that are compatible with those used for the IB model and the system of difference equations (3.2). In particular, the values of the parameters D_n and C_n in the PDE (3.12) are described through the definitions (2.23).

D. Supplementary figures

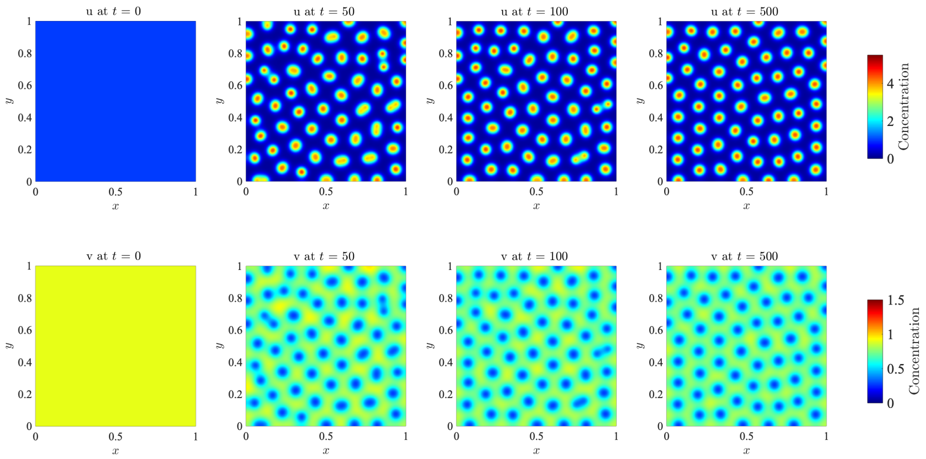

Figure D1. Dynamics of the morphogens on a two-dimensional static domain. Plots of the concentration of activator $u(t, \mathbf{x})$ (top row) and the concentration of inhibitor $v(t, \mathbf{x})$ (bottom row) at four consecutive time instants, obtained by solving numerically the system of PDEs (2.18) for $d = 2$ complemented with the definitions (2.19) and subject to zero-flux boundary conditions. A complete description of the set-up of numerical simulations is given in Appendix B.

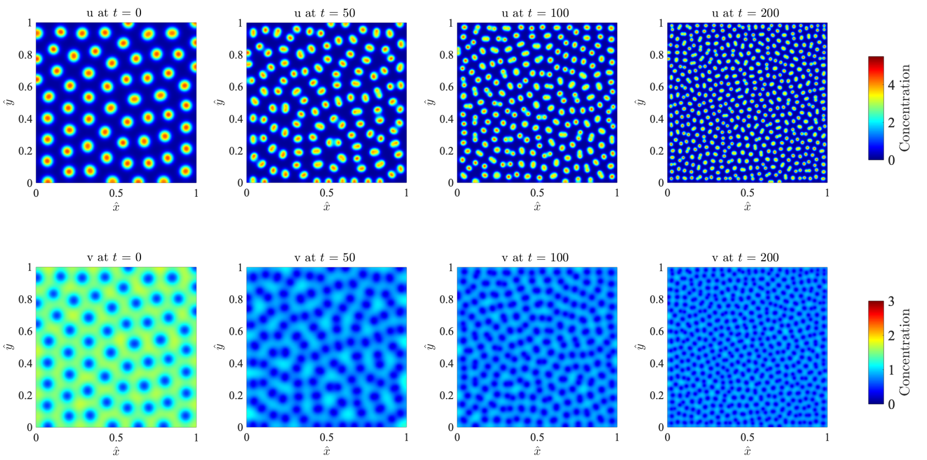

Figure D2. Dynamics of the morphogens on a two-dimensional uniformly growing domain. Plots of the concentration of activator $u(t, \hat{\mathbf{x}})$ (top row) and the concentration of inhibitor $v(t, \hat{\mathbf{x}})$ (bottom row) at four consecutive time instants, obtained by solving numerically the system of PDEs (3.15) for $d = 2$, subject to zero-flux boundary conditions, complemented with the definitions (2.19), Eqs (3.13) and (3.16). A complete description of the set-up of numerical simulations is given in Appendix B.

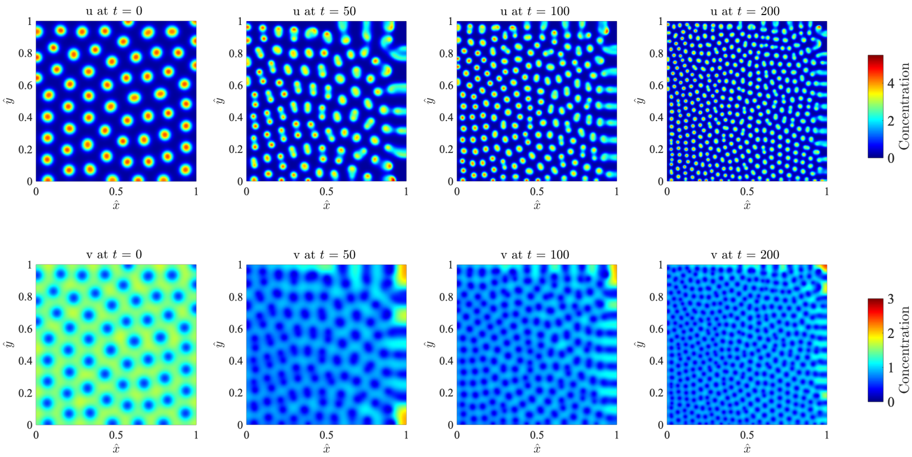

Figure D3. Dynamics of the morphogens on a two-dimensional apically growing domain. Plots of the concentration of activator $u(t, \mathbf{x})$ (top row) and the concentration of inhibitor $v(t, \mathbf{x})$ (bottom row) at four consecutive time instants, obtained by solving numerically the system of PDEs (3.15) for $d = 2$, subject to zero-flux boundary conditions, complemented with the definitions (2.19), Eqs (3.14) and (3.16). A complete description of the set-up of numerical simulations is given in Appendix B.